A Single-Phase Buck–Boost Matrix Converter With Only Six Switches and Without Commutation Problem

Hafiz Furqan Ahmed, Honnyong Cha, *Member, IEEE*, Ashraf Ali Khan, Juyong Kim, and Jintae Cho

***Abstract*—In this paper, a single-phase buck–boost matrix converter is proposed which can both buck and boost the input voltage with step-changed frequency. It consists of only six unidirectional current flowing bidirectional voltage blocking switches, two input and output filter capacitors, and one inductor. It has following advantages over the existing single-phase matrix converters: 1) it can both buck and boost input voltage solving the limited voltage transfer ratio (only boost or buck) problem; 2) it also has enhanced reliability as it is immune from shoot-through problem of voltage source when all switches are turned-on simultaneously, and, therefore, it has no need of PWM dead times and *RC* snubbers or dedicated soft-commutation strategies to solve the commutation problem; 3) it can also use high-speed power MOSFETs as their body diodes never conduct, which eliminate their poor reverse recovery problem. The operation principle of the proposed converter is given, and switching strategies are developed to obtain various multiples and submultiples of input frequency. To verify its performance, a laboratory prototype is fabricated and experiments are performed to produce step-down and step-up voltage with three different frequencies of 120, 60, and 30 Hz.**

***Index Terms*—Buck–boost operation, commutation problem, single-phase matrix converter, step-changed frequency, Z-source.**

I. Introduction

FOR ac–ac power conversions, there are three common traditional converter systems: direct ac–ac converters [1]–[3], indirect ac–dc–ac converters with dc link [4]–[6], and matrix converters (MCs) [7], [9]–[14]. The direct ac–ac converters despite their benefits of single-stage conversion, simple topology, ease of control, and smaller size [8] can only provide voltage regulation and lack the variable frequency operation. Indirect ac–dc–ac converters with dc link can provide both variable output voltage and variable frequency. However, they need a bulky dc-link capacitor and a large-source filter inductor resulting in high cost, large size, high losses, and low reliability [7].

Manuscript received January 26, 2016; revised March 23, 2016; accepted March 29, 2016. Date of publication April 12, 2016; date of current version November 11, 2016. This work was supported by the KEPCO under the project entitled by the "Demonstration Study for Low-Voltage Direct Current Distribution Network in an Island" (D3080). Recommended for publication by Associate Editor R. Redl.

H. F. Ahmed, H. Cha, and A. A. Khan are with the School of Energy Engineering, Kyungpook National University, Daegu 41566, South Korea (e-mail: furqanhmd164@gmail.com; chahonny@knu.ac.kr; 08beeashrafa@seecs.edu.pk).

J. Kim and J. Cho are with the Korea Electric Power Corporation Research Institute, Daejon 34056, South Korea (e-mail: juyong@kepco.co.kr; jintaecho@kepco.co.kr).

Color versions of one or more of the figures in this paper are available online at http://ieeexplore.ieee.org.

Digital Object Identifier 10.1109/TPEL.2016.2553044

The MCs can also provide variable output voltage and frequency with directly connected input power supply to load without intermediate dc-link capacitor. Therefore, they are the best alternative to conventional indirect ac–dc–ac converters with dc link [13]. Owing to their attractive features and huge demand in industrial applications, the MCs have become a hot spot in power electronics with various studies on their modeling and control [15]–[17], topological development [18], [19], and applications [10], [20]. Zuckerberger *et al.* proposed the first single-phase MC [21] with voltage buck and frequency step-up operation. In [22], the experimental study of this single-phase MC is carried out for frequency step-down operation with sinusoidal PWM scheme and *RL* load. A commutation strategy for this single-phase MC is implemented in [23] and [24], to avoid the voltage spikes across switches during dead time. To improve the output power quality of the single-phase MC, modified PWM strategy called staircase modulation is developed in [25] and simulation results are also given to show its advantages. In [26], the application of the single-phase MC for induction heating is proposed, and its comparison with H-bridge converter for the same application is given in [27], which shows its feasibility for induction heating application. In [28], the application of a single-phase MC for driving of induction motor is presented, and experimental results of output voltage, THD, and speed of motor (r/m) are also given which prove that it is the best alternative to replace the dc-link-based ac–dc–ac converter for this application. This single-phase MC is also used to implement a high boost ac–dc MC [29] based on Cockcroft–Walton multiplier, which provides high quality of line conditions, adjustable output voltage, and low output ripple. Nguyen *et al.* proposed the single-phase buck–boost MC [30] based on the existing Z-source topology to use in the applications such as dynamic voltage restorer [31], and to control speed of fan or pump, etc. However, all of these existing single-phase MCs have some drawbacks, such as low-voltage transfer ratio and commutation problem.

1) For the conventional buck MCs [21]–[28], the voltage transfer ratio (ratio between output and input voltage) is limited to <1 with linear modulation [28]. Therefore, they cannot be used for the applications in which the input voltage is required to boost to a higher value. The overmodulation technique can increase the voltage transfer ratio to some extent but at the cost of reducing the quality of both output voltage and input current [32]. On the other hand, the current source MCs [29] can only boost the input voltage and lack the buck operation. To overcome limited voltage transfer ratio, a single-phase Z-source MC has

been proposed in [30], which can provide wide range of buck–boost voltage transfer ratio. However, it uses extra passive components for energy storage (two inductors and two capacitors) and ten active switches, which increases the cost and decreases the power density.

2) All of the single-phase conventional and Z-source MCs [21]–[31] suffer from commutation problem which occurs because of inherent dead time or overlap time between complementary switches, due to different time delays and limited speed of switching devices. During the overlap or dead time, the shoot-through of voltage source or open-circuit of inductor can occur, which may damage switching devices because of excess current or voltage, respectively. In order to solve this commutation problem in a single-phase MC for induction motor drive [28], the authors used dead-time between complementary switches to solve the overlap (short-circuit) problem, and then used *RC* snubbers across each active switch to provide a current path for inductor current during dead time and avoid the switch voltage spikes. However, these bulky and lossy snubbers increase the system cost and decrease the power density and efficiency. The safe-commutation strategies for single-phase conventional MCs are developed in [23] and [24], while for Z-source MC is developed in [30], which provide current path during PWM dead times to avoid voltage overshoot across switches. However, these soft-commutation strategies increase control complexity of the circuits. Moreover, all of these existing single-phase MCs [21]–[31] are hard switching with current also flowing through body diodes of their active switches. Therefore, they cannot utilize high-speed power MOSFETs due to poor reverse-recovery problem of body diodes of MOSFETs [33].

To overcome the aforementioned limited voltage transfer ratio and commutation problem of the existing single-phase MCs, this paper proposes a single-phase MC which can provide buck and boost operations of the input voltage with step-changed frequency. The proposed single-phase MC uses one inductor, two input and output filter capacitors, and six unidirectional conducting bidirectional voltage blocking switches. Compared to the Z-source single-phase MC with ten active switches and four passive components (two inductors and two capacitors for energy storage), the proposed MC uses only six active switches and one inductor (for energy storage), and yet it can provide buck–boost function of input voltage; thus, eliminates the limited voltage transfer problem of the conventional single-phase MCs (buck and boost types). Compared to the existing single-phase MCs, it has no short-circuit problem of voltage source even when all switches are turned on simultaneously; thus, it is highly reliable without the need of PWM dead time and dedicated soft-commutation strategies to solve the commutation problem. Therefore, the proposed single-phase MC can be used to replace the existing single-phase MCs in applications, such as to control the speed of fan, to drive induction motor, to implement induction heating system, and high gain ac–dc MC based on Cockcroft–Walton multiplier, etc. To prove the effectiveness of the proposed buck–boost MC, a hardware prototype is built for output voltage of 70-V rms and experimental results are provided under buck and boost voltage modes with three different frequencies of 60 (same frequency), 30 (step-down), and 120 Hz (step-up).

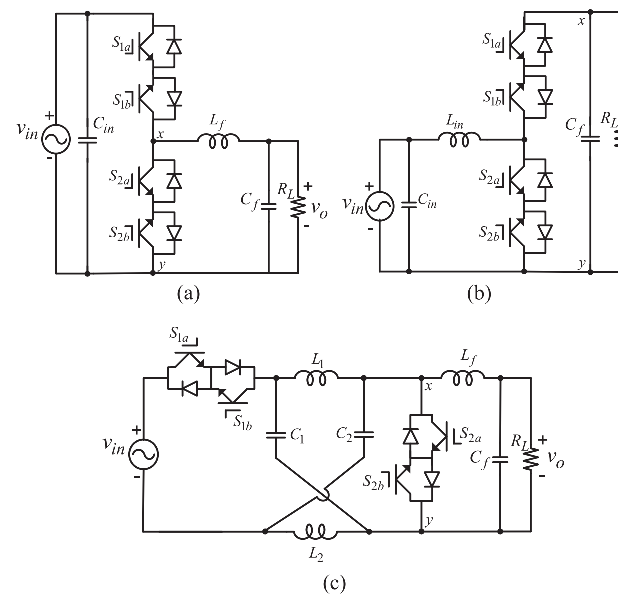

Fig. 1. Single-phase direct PWM ac–ac converters. (a) Buck type [1]. (b) Boost type [1]. (c) Z-source buck–boost type [2].

II. Existing Single-Phase MCs

All of the single-phase PWM ac–ac converters can change the magnitude of input ac voltage by varying the duty ratio D. However, the frequency of input ac voltage fed from grid is fixed (50 or 60 Hz), while there are many single-phase ac–ac conversion applications as described earlier, which require ac voltage with variable frequency. In order to provide ac voltage with variable (step-changed) frequency, the single-phase ac–ac converters are required to operate in both noninverting (provide output voltage which is in-phase with input ac voltage) and inverting (output voltage out-of-phase with input ac voltage) modes for specific time intervals. However, the single-phase direct ac–ac converters (which are obtained from their dc–dc counterparts by replacing each switch and diode with bidirectional switch) cannot change the frequency of ac voltage as they can either provide noninverting or inverting output voltage but not both.

Fig. 1(a)–(c) shows the single-phase buck [1], boost [1], and Z-source buck–boost [2] direct PWM ac–ac converters with voltage gain of D, $1/(1-D)$, and $(1-D)/(1-2D)$, which can produce output voltage with variable magnitude by changing the duty ratio D. However, these buck and boost converters can only produce noninverting output voltage and cannot provide inverting output voltage. The Z-source buck–boost ac–ac converter provide only noninverting output during boost mode (when $D < 0.5$), while only inverting output during buck-mode operation ($D > 0.66$). Therefore, these single-phase direct ac–ac converters cannot change the frequency of output voltage.

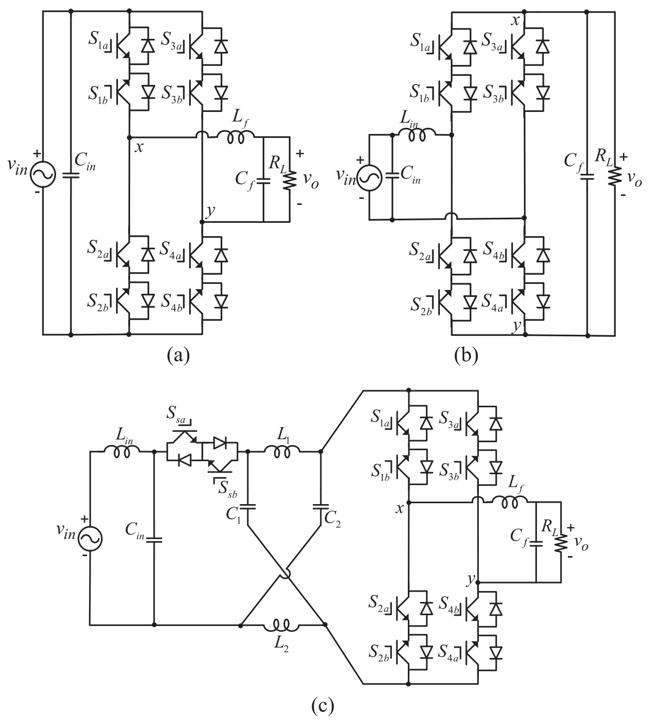

Fig. 2. Existing single-phase MC topologies. (a) Buck MC [23], [24]. (b) Boost MC [29]. (c) Z-source buck–boost MC [30].

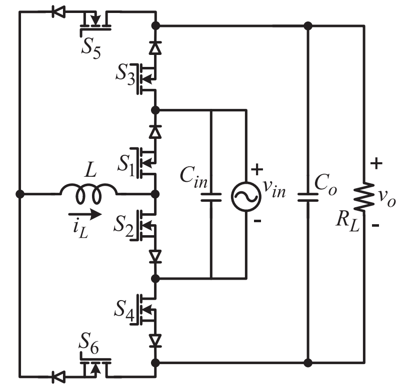

Fig. 3. Circuit topology of the proposed single-phase buck–boost MC.

To overcome this limitation, single-phase buck [23], [24], boost [29], and Z-source buck–boost [30] MCs as shown in Fig. 2(a)–(c) are developed from their direct ac–ac counterparts [shown in Fig. 1(a)–(c)] by adding additional active switches. The single-phase buck and boost MCs shown in Fig. 2(a) and (b) are derived from their direct counterparts in Fig. 1(a) and (b), respectively, by adding an additional bidirectional phase leg consisting of bidirectional switches $S_{3a,3b}$ and $S_{4a,4b}$. While, the Z-source MC as shown in Fig. 2(c) is obtained from its direct counterpart in Fig. 1(c), by replacing the bidirectional switch $S_{2a,2b}$ with two bidirectional phase legs consisting of four bidirectional switches $S_{1a,1b}$–$S_{4a,4b}$. By adding the extra bidirectional phase legs, these single-phase MCs have the capability to provide both noninverting and inverting output voltages. For example, compared to the single-phase buck ac–ac converter [in Fig. 1(a)] where the voltage ν_{xy} (voltage across output *LC* filter) is always in-phase with input voltage $\nu_{\rm in}$ (when switch $S_{1a,1b}$ is ON); the voltage ν_{xy} in single-phase buck MC [shown in Fig. 2(a)] is in-phase with $\nu_{\rm in}$ only when switches $S_{1a,1b}, S_{4a,4b}$ are turned ON, while it is out-of-phase with $\nu_{\rm in}$ when switches $S_{2a,2b}, S_{3a,3b}$ are turned ON. Therefore, by properly selecting the time intervals during which these buck, boost, and Z-source MCs operate in noninverting and inverting modes, the frequency of their output voltage can be changed in steps and multiples and submultiples of input frequency can be obtained. However, these existing single-phase MCs have some limitations and disadvantages as explained:

1) The single-phase buck and boost MCs can only provide buck and boost voltage operation, respectively, and cannot be used in applications which require both buck and boost voltage operation. The Z-source buck–boost MC can provide both buck and boost voltage operations; however, it uses two extra active switches, capacitors C_1, C_2, and inductors L_1, L_2, which increase the cost, size, and losses.
2) All of these three MCs have commutation problem because of inherent dead or overlap time between complementary switches. During overlap time when all switches are turned ON, the buck and boost MCs have short-circuit of input voltage (or $C_{\rm in}$) and output voltage (or C_o), respectively, while the Z-source MC have a short-circuit path containing $C_{\rm in} - S_{\rm sa,sb} - C_1 - S_{2a,2b} - S_{1a,1b} - C_2$, as can be seen in Fig. 2(a)–(c). Therefore, excessive current will flow through active switches which may destroy them. While during dead time when all switches are turned OFF, there is no path for the flow of inductors L_f currents for the buck and Z-source buck–boost MCs, and inductor $L_{\rm in}$ current for boost MC. Therefore, large-voltage spikes will generate across active switches which may also damage them. To overcome this problem, dedicated safe-commutation strategies are used for these MCs in which PWM dead times are deliberately added between complementary switches (to avoid short-circuit problem), and then auxiliary switches are turned ON which provide paths for inductor currents during dead times to avoid switch voltage spikes. These soft-commutation strategies increase the complexity of switching signals and control of the MCs. Moreover in these MCs, body diodes of switches also conduct significant current, and, therefore, they cannot employ high-speed power MOSFETs because of poor reverse-recovery problem of body diodes of MOSFETs.

III. Proposed Single-Phase Buck–Boost MCs

Fig. 3 shows the circuit topology of the proposed single-phase buck–boost MC converter consisting of six unidirectional current flowing bidirectional voltage blocking switches S_1–S_6, one inductor L, and two input and output filter capacitors $C_{\rm in}$ and C_o. We have already introduced this circuit in [34] and [35], where the operation of this circuit as a traditional buck, boost, and inverting buck–boost converters with voltage gain of

D and $1/(1-D)$ and $-D/(1-D)$ were proposed. However, that research was limited to fixed frequency (single 60 Hz) operation of the proposed circuit as conventional noninverting buck and boost converters with voltage gains of D and $1/(1-D)$, respectively, and its comparison with conventional eight switches noninverting buck–boost ac–ac converter with same voltage gains. While in this paper, the buck (D) and boost ($1/(1-D)$) modes of the proposed circuit are completely discarded and instead, new noninverting buck–boost operating mode with voltage gain of $D/(1-D)$ is proposed. In addition, based on this new noninverting buck–boost mode with voltage gain $D/(1-D)$ proposed in this paper, and inverting buck–boost mode with voltage gain $-D/(1-D)$ (proposed in [34] and [35]), various switching strategies are proposed to operate the proposed circuit as a single-phase buck–boost MC with step-changed frequency, and experimental results with three different frequencies are also provided. The proposed single-phase MC has the same variable frequency operation and output voltage as the existing single-phase MCs [21]–[31] with additional benefits, such as both buck and boost operation of input voltage, and no shoot-through problem of voltage source, etc.

Consider the case in which all switches of the proposed MC in Fig. 3 are turned ON simultaneously, resulting in many paths for current to flow. However, there are three paths which can cause the shoot-through of voltage source only if the current can flow through them: 1) Path containing input voltage source and switches S_1, S_2. 2) Path containing output voltage ν_o and switches S_5, S_6. 3) Path containing input and output voltage and switches S_3, S_4. However, all the three paths contain two unidirectional switches in opposite (antiseries) direction, and, therefore, the current cannot flow in these close paths. Hence, the proposed single-phase MC is immune from shoot-through problem which increase its reliability and eliminate the need for dead time along with RC snubbers or soft-commutation strategy, which are required in case of the all existing single-phase MCs [22]–[31].

IV. Circuit Operation and Switching Strategies for Variable Frequency Operation

A. 60-Hz (Same Frequency, $f_o = f_{\mathrm{in}}$) Noninverting Buck–Boost Operation

Fig. 4 shows the gating signals and key waveforms of the proposed converter for noninverting and inverting buck–boost mode operations when output voltage frequency is 60 Hz.

From this figure, it can be seen that during positive half cycle of input voltage ($\nu_{\mathrm{in}} > 0$) for noninverting buck–boost mode, the switches S_1, S_3, S_6 are turned-on while switch S_4 is turned-off completely. The switches S_2, S_5 are high-frequency switches with their on-time and off-time representing time intervals DT and $(1-D)T$, respectively. The equivalent circuit during DT interval is shown in Fig. 5(a), in which the input energy is stored in inductor L.

The series diodes of switches S_1, S_6 are reverse biased, preventing them from conducting the current. Applying KVL yields

$$\nu_L = \nu_{\mathrm{in}}. \tag{1}$$

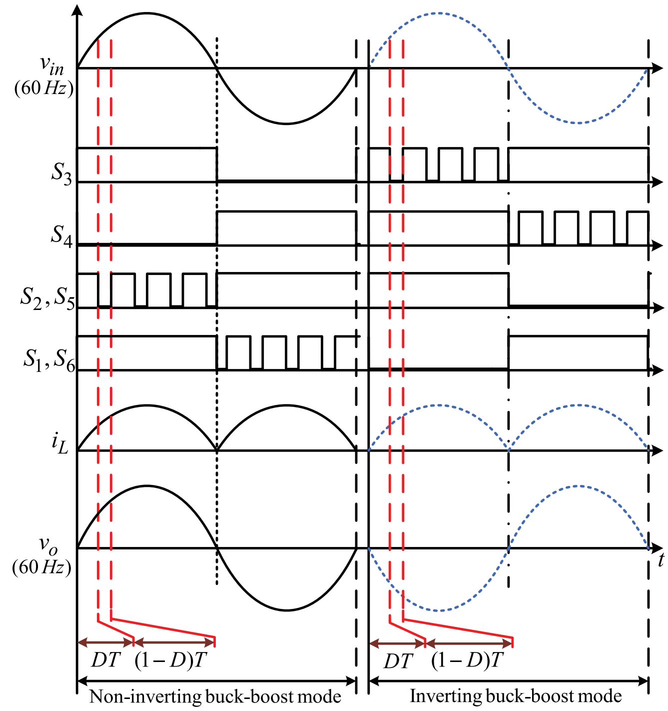

Fig. 4. Switching strategies and key waveforms for noninverting and inverting buck–boost modes.

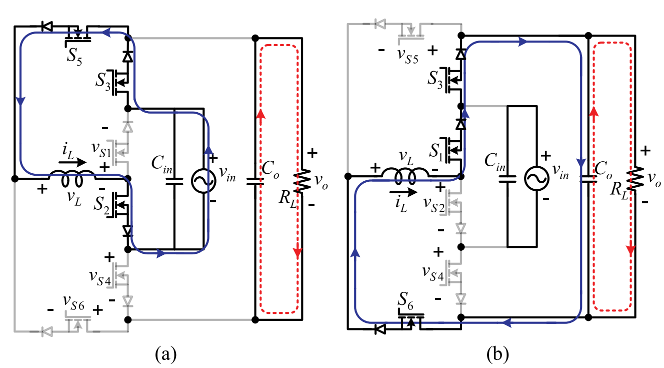

Fig. 5. Noninverting buck–boost operation when $\nu_{\mathrm{in}} > 0$. (a) During DT and (b) during $(1-D)T$.

The equivalent circuit during $(1-D)T$ interval is shown in Fig. 5(b). The switches S_2, S_5 are turned-off during this interval and switches S_1, S_6 conduct current as their series diodes become forward biased to provide free-wheeling path for inductor current. The energy stored in inductor is released to load in this interval. Applying KVL now, gives

$$\nu_L = -\nu_o. \tag{2}$$

Now for negative half cycle of input voltage ($\nu_{\mathrm{in}} < 0$) as shown in Fig. 4, switches S_2, S_4, S_5 are turned-on while switch S_3 is turned-off completely. The equivalent circuits for DT and $(1-D)T$ intervals are shown in Fig. 6(a) and (b), respectively. The circuit operation for $\nu_{\mathrm{in}} < 0$ is similar to that for $\nu_{\mathrm{in}} > 0$, with only difference that now switches S_1, S_6 act same as S_2, S_5 (for $\nu_{\mathrm{in}} > 0$), and vice versa.

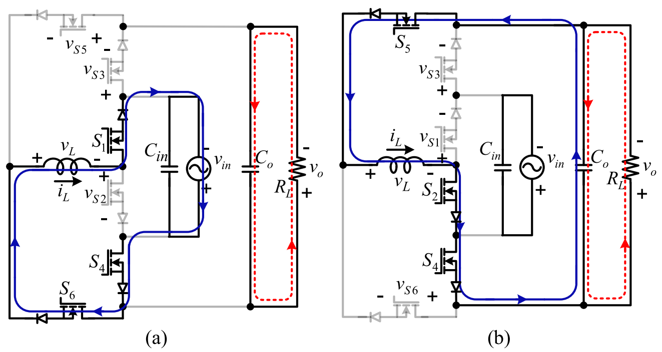

Fig. 6. Noninverting buck–boost operation when $\nu_{\rm in} < 0$. (a) During DT and (b) during $(1-D)T$.

Now, flux balance (volt–sec) balance condition on inductor L using (1) and (2) gives

$$\frac{\nu_o}{\nu_{\rm in}} = \frac{D}{1-D}. \quad (3)$$

From (3), the voltage gain of the proposed converter for this noninverting buck–boost mode is $D/(1-D)$ having voltage buck operation for $D < 0.5$ and boost operation for $D > 0.5$, with same phase and frequency of output voltage as that of input voltage.

B. 60-Hz (Same Frequency, $f_o = f_{\rm in}$) Inverting Buck–Boost Operation

The gating signals and key waveforms during inverting buck–boost mode operation are also shown in Fig. 4. From this figure, it can be seen that in case of inverting buck–boost mode, the gating signal of switch S_3 is same as that of switches S_2, S_5 for noninverting buck–boost operation, and vice versa. While now the switch S_4 has same gating signals as that of switches S_1, S_6 for noninverting buck–boost mode and vice versa. The circuit operation and analysis for this mode is given in [34] and [35]. The voltage gain for this mode is $-D/(1-D)$, with same magnitude as that for noninverting buck–boost mode explained earlier, while the negative sign "$-$" shows that the output voltage is out-of-phase with input voltage as can also be seen in Fig. 4. In [35], the "$-$" sign was not added with voltage gain $D/(1-D)$ during inverting buck–boost mode, because the polarity sign "$\pm$" of voltage ν_o across load R was made reversed in equivalent circuits during this inverting buck–boost mode in [35].

The voltage gain for these noninverting and inverting buck–boost modes are plotted in Fig. 7. The proposed MC can also perform as buck–boost ac–dc rectifier by operating it in noninverting mode for positive half cycle of input voltage and in inverting mode for negative half of input voltage.

C. 30-Hz (Step-Down Frequency, $f_o = (1/2)f_{\rm in}$) Buck–Boost Operation

The switching sequence of the proposed single-phase MC and key waveforms for step-down frequency (from 60 to 30 Hz) operation is shown in Fig. 8. From this figure, it is clear that the step-down frequency operation is performed simply by

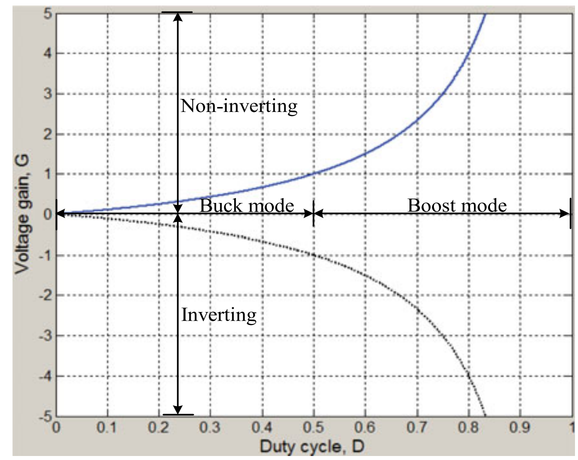

Fig. 7. Voltage gain versus duty ratio for inverting and noninverting buck–boost operation modes.

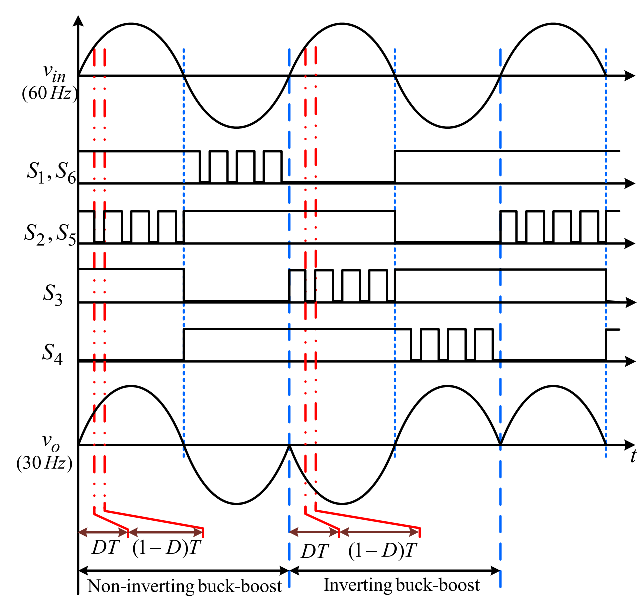

Fig. 8. Switching strategy and waveforms for 30-Hz (step-down, $f_o = (1/2)f_{\rm in}$) frequency operation.

operating the proposed MC in noninverting buck–boost mode for one cycle of input voltage (60 Hz) and then in inverting buck–boost mode in the next cycle, and so on. The switches S_1 and S_6 have same gating signals while switches S_2 and S_5 also have same switching signals. There are no PWM dead times and no soft-commutation strategy used in the switching signals as can be seen in Fig. 8, which enhances the reliability of the proposed MC and makes its switching logic simpler than the existing MCs. The voltage gain in this frequency step-down operation is same $D/(1-D)$ as for 60-Hz (same frequency) operation, with buck-mode operation for $D < 0.5$ and boost-mode operation for $D > 0.5$.

D. 20-Hz (Step-Down Frequency, $f_o = (1/3)f_{\rm in}$) Buck–Boost Operation

The switching sequences and key waveforms for step-down operation of frequency to 20 Hz (1/3 of 60 Hz) is shown in

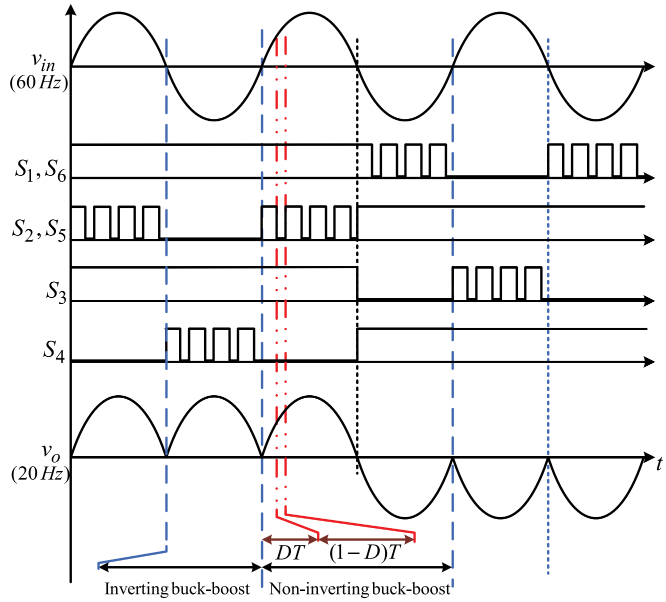

Fig. 9. Switching strategy and waveforms for 20-Hz (step-down, $f_o = (1/3)f_{\text{in}}$) frequency operation.

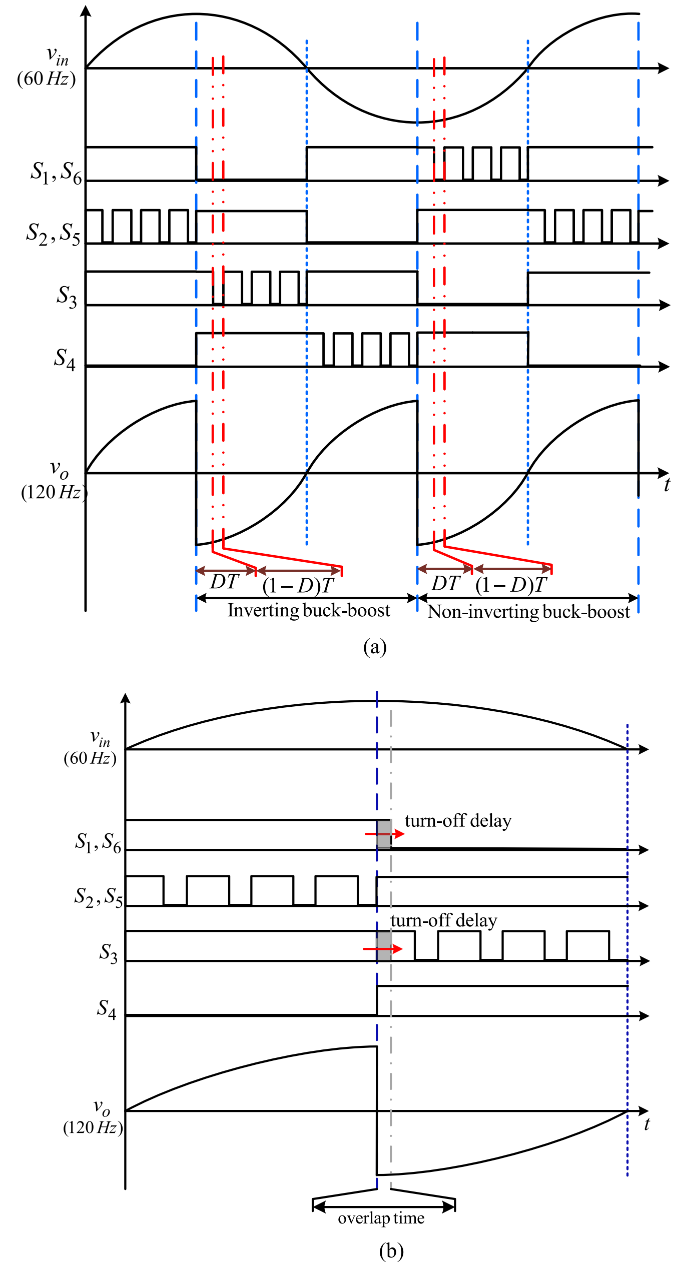

Fig. 10. Switching strategy and waveforms for 120-Hz (step-up, $f_o = 2f_{\text{in}}$) frequency operation. (a) Ideal switching signals. (b) Zoom-in waveforms of (a) for $\nu_{\text{in}} > 0$ with turn-off delay added in low-frequency switches to avoid open-circuit problem of inductor.

Fig. 9. In order to get 1/3 submultiples of input frequency (f_{in}), the proposed single-phase MC is operated in noninverting buck–boost mode for one complete cycle of input voltage and then in inverting buck–boost mode for one half cycle of input voltage, and so on.

E. 120-Hz (Step-Up Frequency, $f_o = 2f_{\text{in}}$) Buck–Boost Operation

The switching sequence of the proposed single-phase MC and key waveforms for step-up frequency (from 60 to 120 Hz) operation is shown in Fig. 10(a). From this figure, it can be seen that the double step-up frequency operation is implemented simply by operating the proposed MC in inverting mode from positive peak to negative peak for half-cycle of input voltage (60 Hz), and then in noninverting mode in the other half cycle from negative to positive peak, and so on. The switches S_1 and S_6 have same gating signals while switches S_2 and S_5 also have same switching signals. The voltage gain in this frequency step-up operation is also same $D/(1-D)$, with buck-mode operation for $D < 0.5$ and boost-mode operation for $D > 0.5$. As have already been mentioned that the proposed MC is immune from shoot-through problem even if all switches are turned-off simultaneously, and, therefore, no dead time is added in its complementary switching signals. However, it is good practice to practically add small turn-off delay in each low-frequency switch which creates a small overlap time between complementary switches during switching transition, and the open-circuit problem of inductor can be avoided. For example, Fig. 10(b) shows the enlarged waveforms of Fig. 10(a) for $\nu_{\text{in}} > 0$ in which small turn-off delay is added in low frequency switches S_1, S_3, and S_6. In this way, an overlap time occurs in switches $S_1 - S_6$ during switching transition, and switches S_2, S_4, and S_5 are always turned-on before switches S_1, S_3, and S_6 are turned-off. Therefore, there is always a path for inductor current to flow and its open-circuit problem is avoided.

F. 180-Hz (Step-Up Frequency, $f_o = 3f_{\text{in}}$) Buck–Boost Operation

The switching sequences and key waveforms for step-up operation of frequency to 180 Hz (three times of 60 Hz) are shown in Fig. 11. In order to get this three times multiple of input frequency (f_{in}), the converter is operated in inverting buck–boost mode for 1/3 of one half-cycle duration, and in noninverting mode for other 2/3 of the half cycle duration, and so on. The

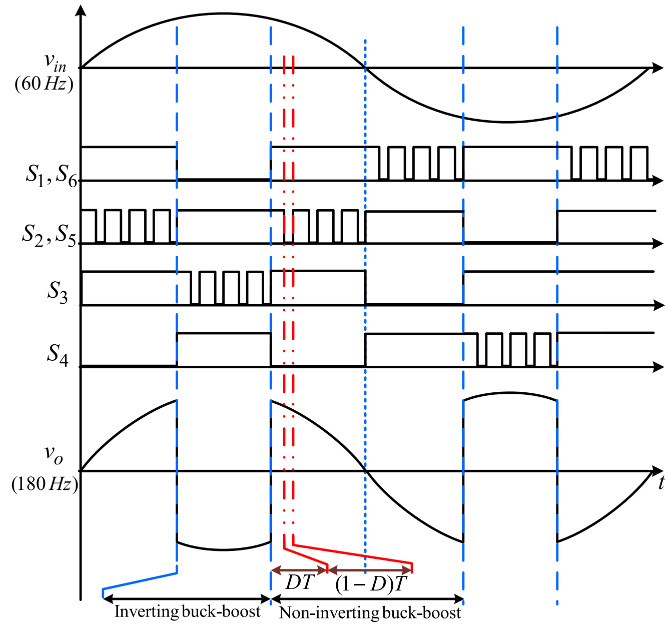

Fig. 11. Switching strategy and waveforms for 180-Hz (step-up, $f_o = 3f_{\rm in}$) frequency operation.

switching patterns of the proposed converter for various frequency operations are also been summarized in Table I, in which T_s represents the time period of input voltage.

From switching sequences of the proposed single-phase buck–boost MC for various frequency modes as shown in Figs. 4, 8–11, it can be noticed that the switches S_1 and S_6 always have same switching signals while S_2 and S_5 also have same switching signals. Therefore, only four different signals are needed to generate for the proposed converter for each frequency operation, compared to ten different signals in case of the single-phase Z-source MC [30], which make the PWM switching strategy much easier for the proposed converter. In addition, no dead times and soft-commutation strategy is needed in switching signals of the proposed single-phase MC as compared to the single-phase conventional MCs and Z-source MC, making the realization of PWM gating signals more simple.

TABLE I
SWITCHING SEQUENCES FOR VARIOUS FREQUENCY MODES

f_{in}	f_o	Time interval	v_{in}	Switch "on" states: Interval, DT	Switch "on" states: Interval, (1-D)T
60 Hz	60 Hz (Inverting)	$0 \sim T_s/2$	>0	S_2, S_3, S_4, S_5	S_2, S_4, S_5
		$T_s/2 \sim T_s$	<0	S_1, S_3, S_4, S_6	S_1, S_3, S_6
	60 Hz (Non-Inverting)	$0 \sim T_s/2$	>0	S_1, S_2, S_3, S_5, S_6	S_1, S_3, S_6
		$T_s/2 \sim T_s$	<0	S_1, S_2, S_4, S_5, S_6	S_2, S_4, S_5
	180 Hz	$0 \sim T_s/6$	>0	S_1, S_2, S_3, S_5, S_6	S_1, S_3, S_6
		$T_s/6 \sim T_s/3$		S_2, S_3, S_4, S_5	S_2, S_4, S_5
		$T_s/3 \sim T_s/2$		S_1, S_2, S_3, S_5, S_6	S_1, S_3, S_6
		$T_s/2 \sim 2T_s/3$	<0	S_1, S_2, S_4, S_5, S_6	S_2, S_4, S_5
		$2T_s/3 \sim 5T_s/6$		S_1, S_3, S_4, S_6	S_1, S_3, S_6
		$5T_s/6 \sim T_s$		S_1, S_2, S_4, S_5, S_6	S_2, S_4, S_5
	120 Hz	$0 \sim T_s/4$	>0	S_1, S_2, S_3, S_5, S_6	S_1, S_3, S_6
		$T_s/4 \sim T_s/2$		S_2, S_3, S_4, S_5	S_2, S_4, S_5
		$T_s/2 \sim 3T_s/2$	<0	S_1, S_3, S_4, S_6	S_1, S_3, S_6
		$3T_s/2 \sim T_s$		S_1, S_2, S_4, S_5, S_6	S_2, S_4, S_5
	30 Hz	$0 \sim T_s/2$	>0	S_1, S_2, S_3, S_5, S_6	S_1, S_3, S_6
		$T_s/2 \sim T_s$	<0	S_1, S_2, S_4, S_5, S_6	S_2, S_4, S_5
		$T_s \sim T_s + T_s/2$	>0	S_2, S_3, S_4, S_5	S_2, S_4, S_5
		$T_s + T_s/2 \sim 2T_s$	<0	S_1, S_3, S_4, S_6	S_1, S_3, S_6
	20 Hz	$0 \sim T_s/2$	>0	S_1, S_2, S_3, S_5, S_6	S_1, S_3, S_6
		$T_s/2 \sim T_s$	<0	S_1, S_3, S_4, S_6	S_1, S_3, S_6
		$T_s \sim T_s + T_s/2$	>0	S_1, S_2, S_3, S_5, S_6	S_1, S_3, S_6
		$T_s + T_s/2 \sim 2T_s$	<0	S_1, S_2, S_4, S_5, S_6	S_2, S_4, S_5
		$2T_s \sim 2T_s + T_s/2$	>0	S_2, S_3, S_4, S_5	S_2, S_4, S_5
		$2T_s + T_s/2 \sim 3T_s$	<0	S_1, S_2, S_4, S_5, S_6	S_2, S_4, S_5

V. Comparison of Inductor Current Ripples and Stresses of Switches for Single-Phase Proposed and Z-Source Buck–Boost MCs

As mentioned earlier, the single-phase buck and boost MCs lack voltage boost and buck operations, respectively, and, therefore, cannot be used for applications requiring both boost and buck operations of input voltage. While both the single-phase proposed and Z-source MCs have buck–boost voltage ability, and, therefore, are potential candidates for applications which need buck and boost operation of input voltage with step-changed frequency. In this section, the component stresses of proposed and Z-source MCs are compared for the application with same output voltage V_o (rms value), output power P_o (rms value), and switching time period T. The input voltage is assumed to be varying from minimum value of $V_{\rm in,min} = V_o/2$ for boost-mode operation to a maximum value of $V_{\rm in,max} = 2V_o$ during buck-mode operation.

1) Apart from filtering components, the Z-source buck–boost MC uses four passive components for energy storage including two capacitors (C_1, C_2) and two inductors (L_1, L_2), while the proposed buck–boost MC uses only one inductor L. Therefore, the proposed MC can save two capacitors and one inductor compared to the Z-source buck–boost MC. The maximum current ripples for inductors L of the proposed and L_1, L_2 of the Z-source MCs, occur during buck mode when input voltage is maximum $V_{\rm in,max}$, and are given by

$$\Delta i_{L\max,\text{proposed}} = \frac{\sqrt{2}V_{\rm in,max}}{L} DT \tag{4}$$

$$\Delta i_{L\max,Z-\text{source}} = \frac{\sqrt{2}V_{\rm in,max}(1-D)}{L(1-2D)} DT. \tag{5}$$

When input voltage is maximum $V_{\rm in,max}$, the voltage gain ($V_o/V_{\rm in,max}$) is 0.5. To obtain this gain, the duty ratio D values for the proposed and Z-source MCs are 0.33 and 0.75, respectively. By putting these values of D in (4) and (5) and solving the maximum inductor current ripples become

$$\Delta i_{L\max,\text{proposed}} = 0.333 \times \left(\frac{\sqrt{2}V_{\text{in,max}}}{L}T\right) \quad (6)$$

$$\Delta i_{L\max,Z\text{-source}} = 0.375 \times \left(\frac{\sqrt{2}V_{\text{in,max}}}{L}T\right). \quad (7)$$

From (6) and (7), it is clear that for the same inductance value *L*, the inductor *L* in the proposed MC has slightly lower current ripple compared to that of the inductors L_1 and L_2 of the Z-source MC. Therefore, to maintain the same current ripple, the inductor *L* in the proposed MC require slightly lower inductance value compared to that of the each inductor L_1 and L_2 of the Z-source MC.

2) Compared to the Z-source buck–boost MC which uses ten active switches, the proposed buck–boost MC uses six unidirectional current conducting and bidirectional voltage blocking switches which are either realized by connecting six MOSFETs in series with external diodes, or by using six reverse-blocking IGBTs. In this section, the maximum voltage and current stresses of active switches are compared for both the proposed and Z-source MCs.

The maximum voltage stress across switches occurs during buck mode when $V_{\text{in}} = V_{\text{in,max}}$ and given by for two MCs as

$$\begin{cases} V_{\text{S1,S2(max)-proposed}} = \sqrt{2}V_{\text{in,max}} = 2\sqrt{2}V_o \\ V_{\text{S5,S6(max)-proposed}} = \sqrt{2}V_o \\ V_{\text{S3,S4(max)-proposed}} = \sqrt{2}V_{\text{in,max}} = 3\sqrt{2}V_o \end{cases} \quad (8)$$

$$\begin{cases} V_{\text{Sxa,Sxb(max)}-Z\text{-source}} = \dfrac{\sqrt{2}V_{\text{in,max}}}{1-2D} = \dfrac{2\sqrt{2}V_o}{1-2D} \\ \text{where } x = s,1,2,3,4. \end{cases} \quad (9)$$

Putting the value of $D = 0.75$ (to get a gain of $V_o/V_{\text{in,max}} = 0.5$) in (9), we get

$$\begin{cases} V_{\text{Sxa,Sxb(max)}-Z\text{-source}} = 4\sqrt{2}V_o \\ \text{where } x = s,1,2,3,4. \end{cases} \quad (10)$$

From (8) and (10), it can be seen that for the proposed MC, the maximum voltage stress of switches S_1, S_2 are 1/2, switches S_5, S_6 are 1/4, and switches S_3, S_4 are 3/4 times lower than that of all the ten switches in the Z-source MC. Therefore, compared to the Z-source MC, the proposed MC can uses switches with lower voltage ratings and also can reduce the switching losses.

The maximum current passes through switches of both the MCs during boost mode when $V_{\text{in}} = V_{\text{in,min}}$ (and $I_{\text{in}} = I_{\text{in,max}}$), and given as (ignoring current ripple)

$$\begin{cases} I_{Sy,\max-\text{proposed}} = \sqrt{2}\left(\dfrac{P_o}{V_{\text{in,min}} + V_o}\right) = \dfrac{3\sqrt{2}P_o}{V_o} \\ y = 1,2,3,4,5,6. \end{cases} \quad (11)$$

$$\begin{cases} I_{Sx,sb(\max)-Z\text{-source}} = \dfrac{\sqrt{2}P_o}{(1-D)V_{\text{in,min}}} = \dfrac{2\sqrt{2}P_o}{(1-D)V_o} \\ x = s,1,2,3,4. \end{cases} \quad (12)$$

Putting the value of $D = 1/3$ (to get a gain of $V_o/V_{\text{in,min}} = 2$) in (12), we get

$$\begin{cases} I_{Sx,sb(\max)-Z\text{-source}} = \dfrac{\sqrt{2}P_o}{(1-D)V_{\text{in,min}}} = \dfrac{3\sqrt{2}P_o}{V_o} \\ x = s,1,2,3,4. \end{cases} \quad (13)$$

From (11) and (13), it is clear that the current ratings of all the switches in proposed MC are same as that of all the switches in the Z-source MC.

Therefore, the proposed buck–boost MC has benefits in that it has slightly lower inductor current ripple, and also it can use switches with same current but lower voltage ratings compared to that in the Z-source buck–boost MC.

VI. Loss Consideration of the Proposed Buck–Boost MC

Apart from input and output filtering capacitors which have negligible power loss, the main losses in the proposed MC consists of semiconductor switching devices losses and energy storing component losses.

A. *Semiconductor Switching Devices Losses*

The losses in switching devices are the major losses in the proposed MC. The proposed MC uses six active switches $S_1 - S_6$ and six external diodes $D_1 - D_6$. As the body diodes of active switches do not conduct current, it uses high-speed power MOSFETs as active switches. The switching device (MOSFETs and external diodes) losses come from switching and conduction loss of MOSFETs, and reverse recovery and forward voltage drop loss of external diodes.

In the proposed MC, during inverting buck–boost mode, only one MOSFET (S_3 or S_4) and one diode (D_3 or D_4) with voltage stress of $\nu_{\text{in}} + \nu_o$ are switched at high frequency at a time. While during noninverting buck–boost mode, two MOSFETs (S_1, S_6 or S_2, S_5) and two external diodes (D_1, D_6 or D_2, D_5) are switched at high frequency at a time with voltage stress of ν_{in} for MOSFETs S_1, S_2 (and D_1, D_2) and ν_o for MOSFETs S_2, S_5 (and diodes D_5, D_6). The main switching losses of MOSFETs and reverse-recovery losses of external diodes come from these high-frequency switching MOSFETs and diodes, while there will be some minor switching and reverse recovery losses from low-frequency MOSFETs and external diodes, respectively. As the proposed MC uses high-speed MOSFETs with external fast recovery diodes, its switching and reverse recovery losses will be smaller than those of the conventional MCs constructed with IGBTs with body diode.

In the proposed MC, there are three MOSFETs and three external diodes in a current conducting power loop. Therefore, the proposed MC has three MOSFETs conduction losses and three external diodes voltage drop losses. As the use of MOSFETs and external fast recovery diodes decrease the switching and reverse-recovery losses of the proposed MC, these MOSFETs conduction and diode voltage drop losses are the more prominent semiconductor losses. The proposed MC can utilize SiC MOSFETs (as their body diodes never conduct in the proposed MC) with very low R_{ds} on along with external low forward

TABLE II
ELECTRICAL SPECIFICATIONS OF THE PROPOSED SINGLE-PHASE BUCK–BOOST MC

Output voltage	70 $\mathrm{V_{rms}}$
Input voltage (buck mode)	95 $\mathrm{V_{rms}}$
Input voltage (boost mode)	45 $\mathrm{V_{rms}}$
Output power	200 W
Switching frequency	25 kHz
MOSFET ($S_1 - S_6$)	47N60CFD (600 V)
Diode ($D_1 - D_6$)	RHRG3060 (600 V)
Inductor (L)	$800\,\mu$H
Input capacitor ($C_{\rm in}$)	$1.5\,\mu$F
Output capacitor (C_o)	$4.5\,\mu$F

voltage drop diodes to decrease these conduction and voltage drop losses, respectively.

B. Energy Storing Component Losses

The proposed MC uses only one inductor L as energy storing component and the remaining loss of the proposed MC comes from conduction and core loss of this inductor L with winding conduction loss being the dominant one. The design requirement and losses of this inductor L is the same as that of inductor in the conventional inverting buck–boost ac–ac converter under the same switching frequency condition. However, compared to the conventional inverting buck–boost ac–ac converter which uses IGBTs, the switching frequency of the proposed MC can be increased owing to the use of power MOSFETs. Hence, for the same current ripple, the proposed MC can use inductor with smaller inductance value and the winding loss of inductor can be decreased.

VII. Experimental Results

To verify the previous analysis, a 200-W laboratory prototype of single-phase buck–boost MC was built and tested. Table II shows the electrical specifications of the proposed converter. An LEM LV-25P voltage sensor was used to detect the zero crossings, and the sensor signals were sent to TMS320F28335 DSP-kit using 12 bit A/D converter. The DSP kit generated six gating signals for three different frequency operations.

Figs. 12 and 13 show the experimental results of the proposed buck–boost MC for 60-Hz output voltage during noninverting and inverting buck–boost operations, respectively. Fig. 12(a) and (b) shows the input voltage, output voltage, and output current for noninverting boost and buck modes, while Fig. 13(a) and (b) shows these waveforms for inverting boost and buck modes, respectively. Figs. 12(c) and 13(c) show the switch voltage stress for high-frequency switches and inductor current for noninverting and inverting buck modes, respectively, while Figs. 12(d) and 13(d) show zoom-in waveforms of these stresses.

Fig. 14 shows the experimental results for buck and boost modes when output frequency is 30 Hz. Fig. 14(a) and (b) shows the input voltage, output voltage, and output current during boost and buck modes, respectively. Fig. 14(c) shows the switch voltage stress for high-frequency switches and inductor current, while Fig. 14(d) shows zoom-in waveforms of these stresses.

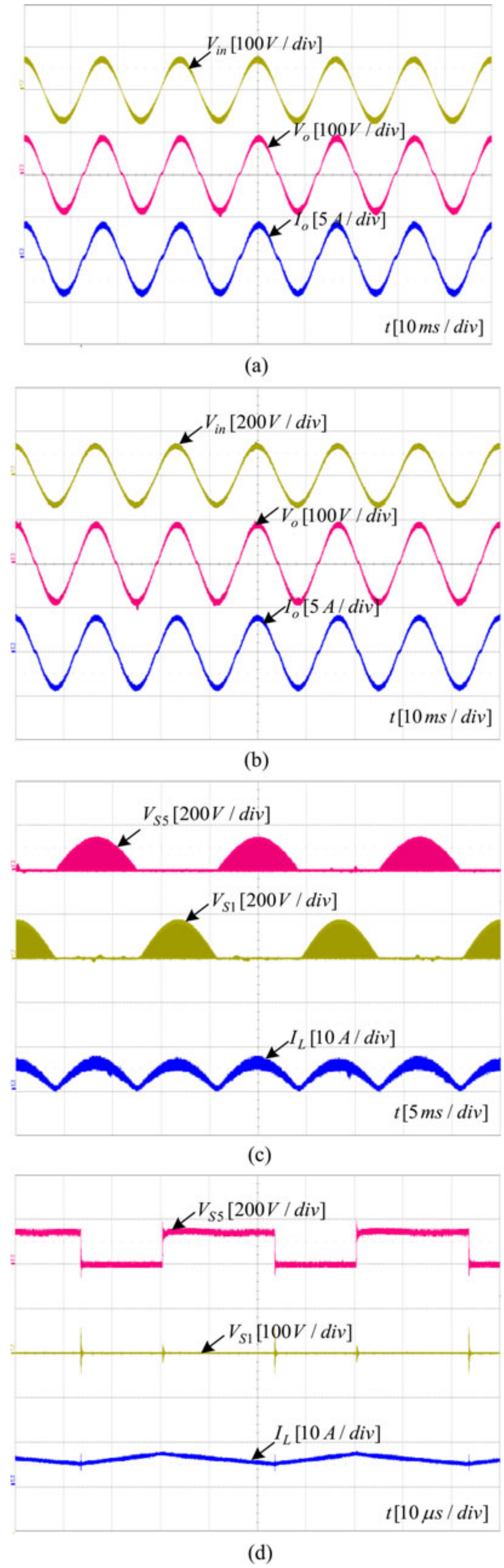

Fig. 12. Experimental results of the proposed ac–ac converter under noninverting buck–boost mode operations for $V_o = 70\ \mathrm{V_{rms}}$ and $f_o = 60\,$Hz. (a) Boost operation when $V_{\rm in} = 45\,\mathrm{V_{rms}}$, $D = 0.61$. (b) Buck operation when $V_{\rm in} = 95\,\mathrm{V_{rms}}$, $D = 0.42$. (c) Components stresses. (d) Zoom-in waveforms of (c).

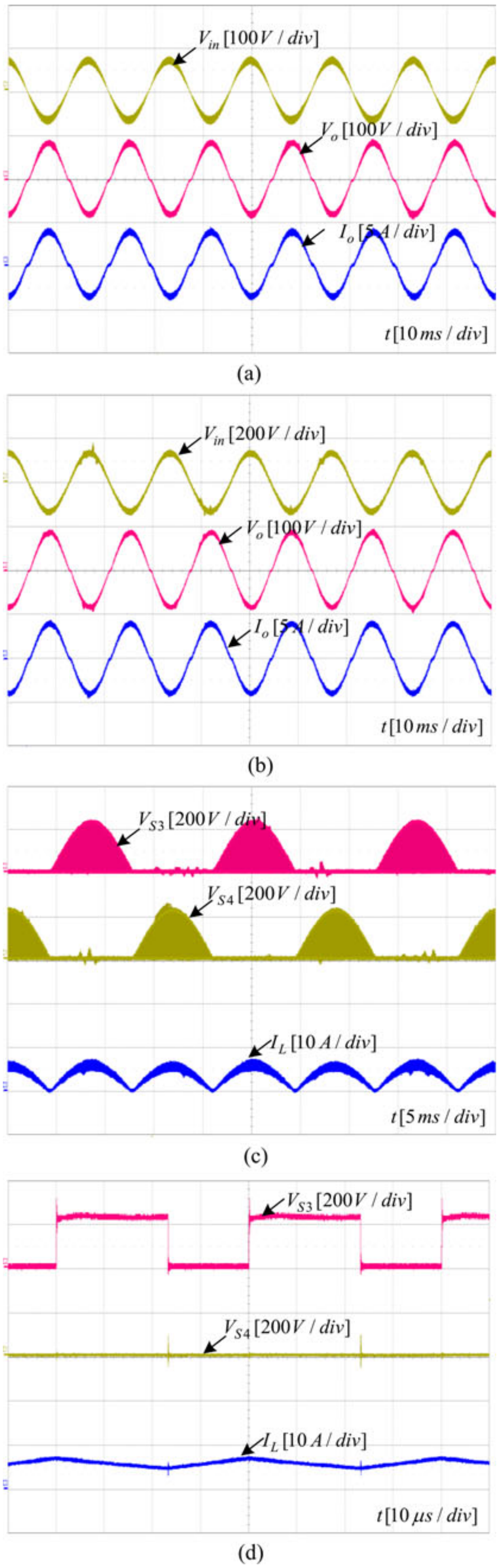

Fig. 13. Experimental results of the proposed ac–ac converter under inverting buck–boost mode operations for $V_o = 70\,\mathrm{V_{rms}}$ and $f_o = 60\,\mathrm{Hz}$. (a) Boost operation when $V_{\mathrm{in}} = 45\,\mathrm{V_{rms}}$, $D = 0.61$. (b) Buck operation when $V_{\mathrm{in}} = 95\,\mathrm{V_{rms}}$, $D = 0.42$. (c) Components stresses. (d) Zoom-in waveforms of (c).

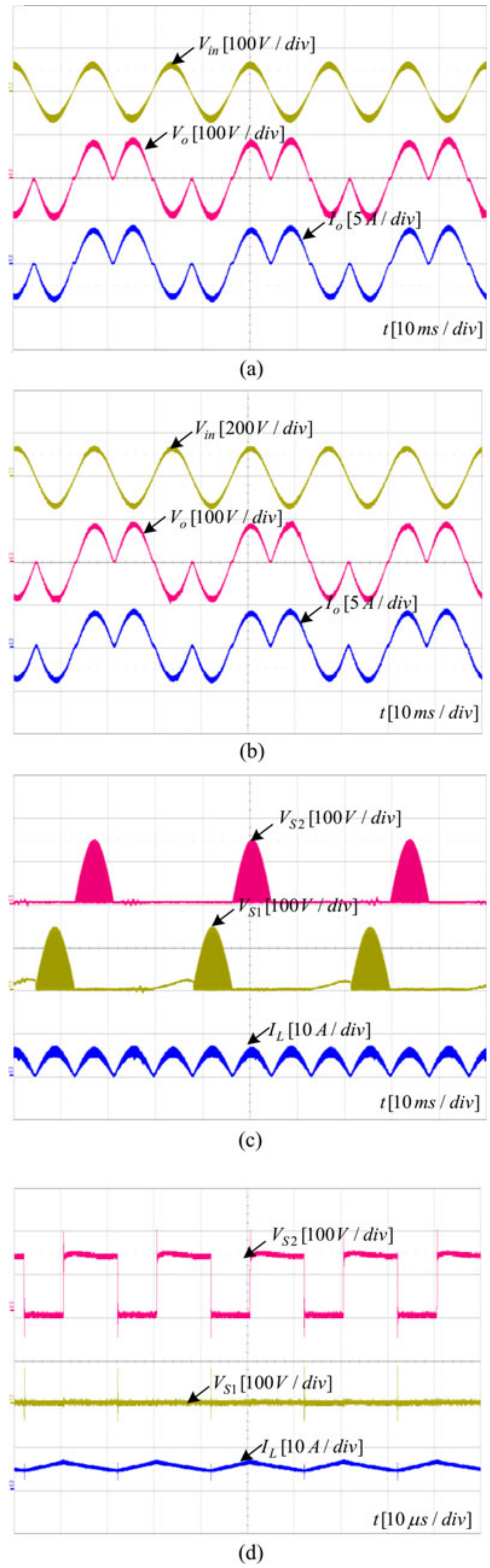

Fig. 14. Experimental results of the proposed ac–ac converter under buck–boost mode operations for $V_o = 70\,\mathrm{V_{rms}}$ and step-down frequency operation when $f_o = 30\,\mathrm{Hz}$. (a) Boost operation when $V_{\mathrm{in}} = 45\,\mathrm{V_{rms}}$, $D = 0.61$. (b) Buck operation when $V_{\mathrm{in}} = 95\,\mathrm{V_{rms}}$, $D = 0.42$. (c) Switch voltage and inductor current stresses. (d) Zoom-in waveforms of (c).

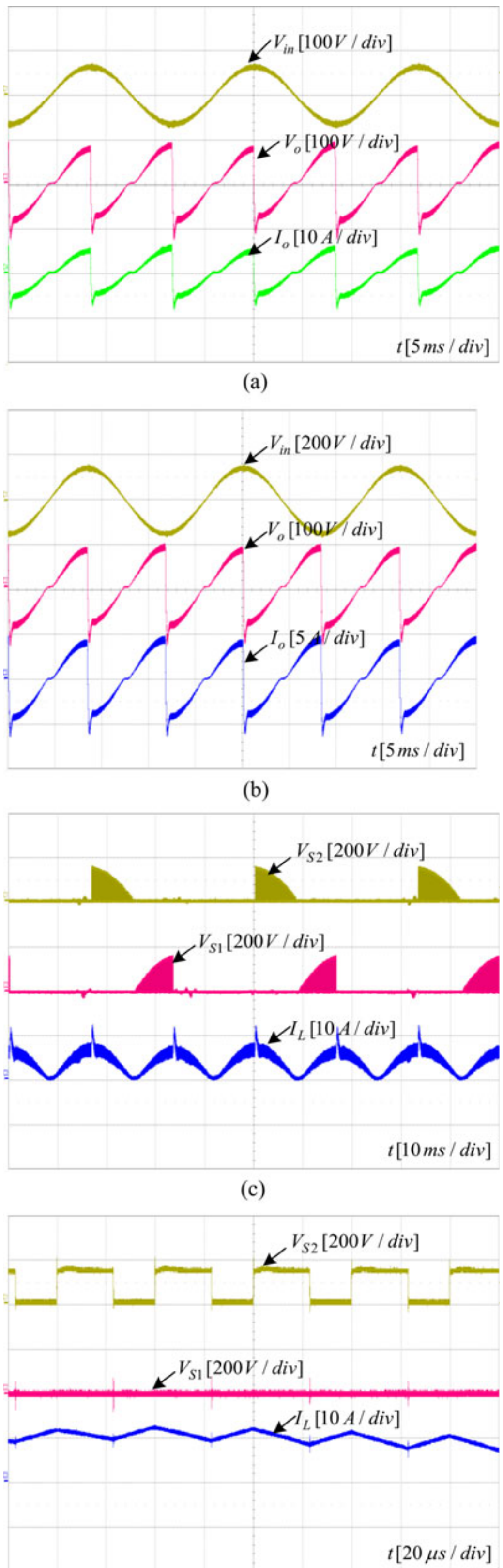

Fig. 15. Experimental results of the proposed ac–ac converter under buck–boost mode operations for $V_o = 70\,\mathrm{V_{rms}}$ and step-up frequency operation when $f_o = 120\,\mathrm{Hz}$. (a) Boost operation when $V_{\mathrm{in}} = 45\,\mathrm{V_{rms}}$, $D = 0.61$. (b) Buck operation when $V_{\mathrm{in}} = 95\,\mathrm{V_{rms}}$, $D = 0.42$. (c) Switch voltage and inductor current stresses. (d) Zoom-in waveforms of (c).

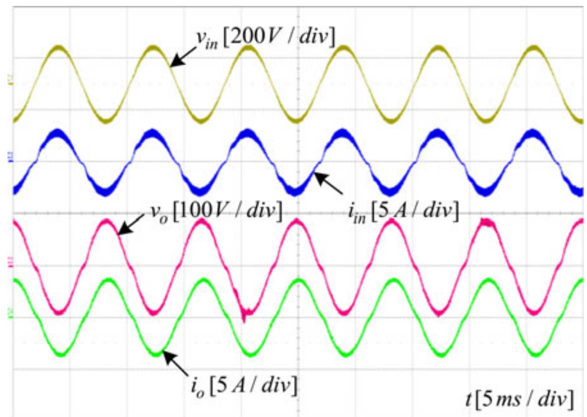

Fig. 16. Experimental waveforms of input voltage ν_{in}, output voltage ν_o, input current i_{in}, and output current i_o during 60-Hz inverting mode operation with inductive load ($R = 30\ \Omega$, $L = 10\,\mathrm{mH}$) when $V_{\mathrm{in}} = 95\,\mathrm{V_{rms}}$, $D = 0.42$.

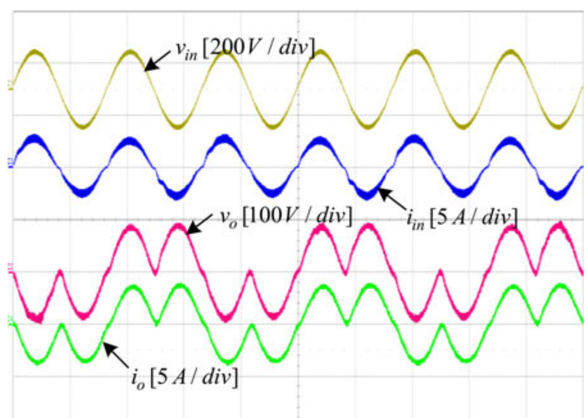

Fig. 17. Experimental waveforms of input voltage ν_{in}, output voltage ν_o, input current i_{in}, and output current i_o during 30-Hz mode operation with inductive load ($R = 30\ \Omega$, $L = 10\,\mathrm{mH}$) when $V_{\mathrm{in}} = 95\,\mathrm{V_{rms}}$, $D = 0.42$.

Fig. 15 shows the experimental results for buck and boost modes when output frequency is 120 Hz. Fig. 15(a) and (b) shows the input voltage, output voltage, and output current during boost and buck modes, respectively. Fig. 15(c) shows the switch voltage stress for high-frequency switches and inductor current, while Fig. 15(d) shows zoom-in waveforms of these stresses.

Figs. 16 and 17 show the experimental results of input and output voltages and currents under 60-Hz inverting mode and 30-Hz modes, respectively, for *RL* load with $R = 30\ \Omega$ and $L = 10$ mH. An input *LC* filter with $L = 0.23$ mH and $C = 1.5\ \mu$F is also used (as have been done for the Z-source buck–boost MC in [30]) to make the input current continuous which can be seen in Figs. 16 and 17.

The efficiency of the proposed single-phase MC is given in Fig. 18 when $V_o = 70\ \mathrm{V_{rms}}$ and $P_o = 200\,\mathrm{W}$. From this figure, it can be seen that the efficiency is maximum when input voltage is maximum (input current is minimum) during buck mode, and it decreases as the input voltage decreases. This is because the conduction losses of MOSFETs and series diodes are dominant losses in the proposed MC, which increases as the input

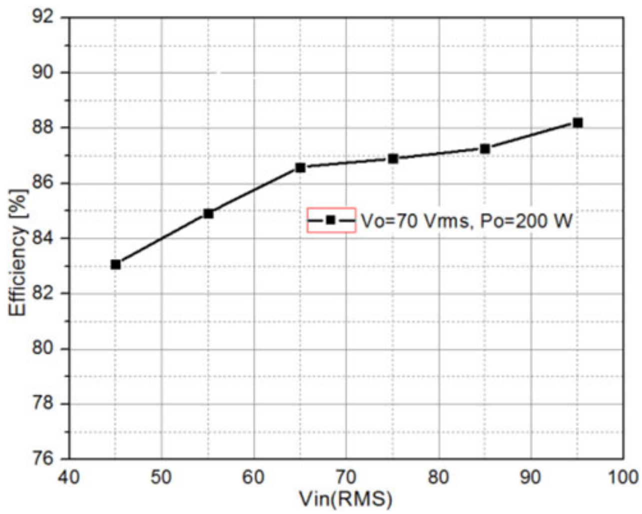

Fig. 18. Efficiency of the proposed single-phase buck–boost MC.

current increases (with decrease in input voltage). The measured efficiency is low as due to limitation in components available in the laboratory, the prototype MC was intended only to verify the operational concept and was not optimized to obtain better efficiency. The prototype of the proposed buck–boost MC is fabricated and experimented for low voltage. However, all the MOSFETs (S_1-S_6) and diodes (D_1-D_6) used in the experiment are of higher voltage rating of 600 V. These high-voltage rating MOSFETs and diodes have relatively higher losses which reduced the measured efficiency of the proposed MC. All of these experimental results are in good agreement with the previous analysis; therefore, validate the advantages of the proposed single-phase buck–boost MC.

VIII. Conclusion

In this paper, a single-phase buck–boost MC is proposed which consists of one inductor, two filter capacitors, and six unidirectional current conducting bidirectional voltage blocking switches. It can step-changed the output frequency with both voltage buck and boost operation; therefore, solves the limited gain (only buck or boost) ability of the existing single-phase MCs. The proposed single-phase MC is more reliable than the existing MCs as it can turn on all switches simultaneously without current overshoot problem caused by the short-circuit of voltage source. Therefore, it does not have commutation problem and eliminates the need for PWM dead times and lossy *RC* snubbers or dedicated soft-commutation strategies, which is a significant advantage.

A detailed analysis of the proposed topology and switching strategies are given for buck–boost operation with step-down same and step-up frequency. A scaled-down laboratory prototype of the proposed MC with output voltage of 70-$V_{\rm rms}$ was fabricated based on TMS320F28335 DPS-kit to generate the control signals, and experimental results under buck and boost modes were given for output frequencies of 30 (step-down frequency), 60 (same frequency), and 120 Hz (step-up frequency). The proposed MC can be used in applications which require voltage regulation along with frequency variation such as to control the speed of a fan or a pump, to drive induction motor, for induction heating, and to implement a high-boost ac–dc MC based on Cockcroft–Walton voltage multiplier, etc.

References

[1] B. H. Kwon, B. D. Min, and J. H. Kim, “Novel topologies of AC choppers,” *Proc. IEE Electr. Power Appl.*, vol. 143, no. 4, pp. 323–330, Jul. 1996.

[2] X. P. Fang, Z. M. Qian, and F. Z. Peng, “Single-phase Z-source PWM ac–ac converters,” *IEEE Power Electron. Lett.*, vol. 3, no. 4, pp. 121–124, Dec. 2005.

[3] T. B. Lazzarin, R. L. Andersen, and I. Barbi, “A switched-capacitor three-phase ac-ac converter,” *IEEE Trans. Ind. Electron.*, vol. 62, no. 2, pp. 735–745, Feb. 2015.

[4] D.-C. Lee and Y.-S. Kim, “Control of single-phase-to-three-phase ac/dc/ac PWM converters for induction motor drives,” *IEEE Trans. Ind. Electron.*, vol. 54, no. 2, pp. 797– 804, Apr. 2007.

[5] J. E. C. D. Santos, C. B. Jacobina, N. Rocha, and E. R. C. D. Silve, “Six-phase machine drive system with reversible parallel ac-dc-ac converters,” *IEEE Trans. Ind. Electron.*, vol. 58, no. 5, pp. 2049–2053, May 2011.

[6] P. Alemi, Y.-C. Jeung, and D.-C. Lee, “DC-link capacitance minimization in T-type three-level ac/dc/ac PWM converters,” *IEEE Trans. Ind. Electron.*, vol. 62, no. 3, pp. 1382–1391, Mar. 2015.

[7] J. W. Kolar, T. Friedli, J. Rodriguez, and P. W. Wheeler, “Review of three-phase PWM ac-ac converter topologies,” *IEEE Trans. Ind. Electron.*, vol. 58, no. 11, pp. 4088–5006, Nov. 2011.

[8] M.-K. Nguyen, Y.-G. Jung, and Y.-C. Lim, “Single-phase ac-ac converter based on quasi-Z-source topology,” *IEEE Trans. Power Electron.*, vol. 25, no. 8, pp. 2200–2209, Aug. 2010.

[9] A. Dasgupta and P. Sensarma, “Filter design of direct matrix converter for synchronous applications,” *IEEE Trans. Ind. Electron.*, vol. 61, no. 12, pp. 6483–6493, Dec. 2014.

[10] R. K. Gupta, K. K. Mohapatra, A. Somani, and N. Mohan, “Direct-matrix-converter-based drive for a three-phase open-end-winding ac machine with advanced features,” *IEEE Power Ind. Electron.*, vol. 57, no. 12, pp. 4032–4042, Dec. 2010.

[11] J. Espina, J. Balcells, A. Arias, and C. Ortega, “Common mode EMI model for a direct matrix converter,” *IEEE Trans. Ind. Electron.*, vol. 58, no. 11, pp. 5049–5056, Nov. 2011.

[12] Y. Sun, X. Li, M. Su, H. Wang, H. Dan, and W. Xiong, “Indirect matrix converter-based topology and modulation schemes for enhancing input reactive power capability,” *IEEE Trans. Power Electron.*, vol. 30, no. 9, pp. 4669–4681, Sep. 2015.

[13] P. C. Loh, F. Blaabjerg, F. Gao, A. Baby, and D. A. C. Tan, “Pulsewidth modulation of neutral-point-clamped indirect matrix converter,” *IEEE Trans. Ind. Electron.*, vol. 44, no. 6, pp. 1805–1814, Nov./Dec. 2008.

[14] T. D. Nguyen and H.-H. Lee, “Dual three-phase indirect matrix converter with carrier-based PWM method,” *IEEE Trans. Power Electron.*, vol. 29, no. 2, pp. 569–581, Feb. 2014.

[15] H. Hojabri, H. Mokhtari, and L. Chang, “A generalized technique of modeling, analysis, and control of a matrix converter using SVD,” *IEEE Trans. Ind. Electron.*, vol. 58, no. 3, pp. 949–959, Mar. 2011.

[16] D. Casadei, J. Clare, L. Empringham, G. Serra, A. Tani, P. Wheeler, and L. Zarri, “Large-signal model for the stability analysis of matrix converters,” *IEEE Trans. Ind. Electron.*, vol. 54, no. 2, pp. 939–950, Apr. 2007.

[17] C. Xia, Y. Yan, P. Song, and T. Shi, “Voltage disturbance rejection for matrix converter-based PMSM drive system using internal model control,” *IEEE Tran. Ind. Electron.*, vol. 59, no. 1, pp. 361–372, Jan. 2012.

[18] C. Klumpner, P. Nielsen, I. Boldea, and F. Blaabjerg, “A new matrix converter motor (MCM) for industry applications,” *IEEE Tran. Ind. Electron.*, vol. 49, no. 2, pp. 325–335, Apr. 2002.

[19] C. Clumpner and F. Blaabjerg, “Modulation method for a multiple drive system based on a two-stage direct power conversion topology with reduced input current ripple,” *IEEE Tran. Power Electron.*, vol. 20, no. 4, pp. 922–929, Nov. 2005.

[20] R. Cardenas, R. Pena, P. Wheeler, J. Clare, and G. Asher, “Control of the reactive power supplied by a WECS based on an induction generator fed by a matrix converter,” *IEEE Tran. Ind. Electron.*, vol. 56, no. 2, pp. 429–438, Feb. 2009.

[21] A. Zuckerberger, D. Weinstock, and A. Alexandrovitz, “Single-phase matrix converter,” *Proc. Inst. Electr. Eng. Electr. Power Appl.*, vol. 144, pp. 235–240, 1997.

[22] Z. Idris and M. K. Hamzah, "Implementation of a new single-phase cycloconverter based on single-phase matrix converter topology using sinusoidal pulse width modulation with passive load condit," in *Proc. IEEE Conf. Ind. Electron. Appl.*, 2006, pp. 1–6.

[23] S. Z. Idris, M. K. Hamzah, and M. F. Saidon, "Implementation of single-phase matrix converter as a direct ac-ac converter with commutation strategies," in *Proc. Conf. Rec. IEEE Power Electron. Spec. Conf.*, 2006, pp. 2240–2246.

[24] Z. Idris, S. Z. M. Noor, and M. K. Hamzah, "Safe commutation strategy in single-phase matrix converter," in *Proc. IEEE 6th Int. Conf. Power Electron. Drive Syst.*, 2005, pp. 886–891.

[25] A. Agarwal and V. Agarwal, "Staircase modulated AC to AC converter," in *Proc. Int. Conf. Power, Control Embedded Syst.*, Dec. 2010, pp. 1–5.

[26] N. Nguyen-Quang, D. A. Stone, C. M. Bingham, and M. P. Foster, "Single phase matrix converter for radio frequency induction heating," in *Proc. Int. Symp. Power Electron. Electr. Drives Autom. Motion*, 2006, pp. S18–28–S18-32.

[27] N. Nguyen-Quang, D. A. Stone, C. Bingham, and M. P. Foster, "Comparison of single-phase matrix converter and H-bridge converter for radio frequency induction heating," in *Proc. Eur. Conf. Power Electron. Appl.*, 2007, pp. 1–9.

[28] S. Sünter and Ö. Aydoğmuş, "Implementation of a single-phase matrix converter induction motor drive," *Springer Electr. Eng.*, vol. 90, no. 6, pp. 425–433, 2008.

[29] C.-M. Young, H.-L. Chen, and M.-H. Chen, "A Cockcroft-walton voltage multiplier fed by a three-phase-to-single phase matrix converter with PFC," *IEEE Trans. Ind. Appl.*, vol. 50, no. 3, pp. 1994–2004, May/Jun. 2014.

[30] M.-K. Nguyen, Y.-G. Jung, Y.-C. Lim, and Y.-M. Kim, "A single-phase Z-source buck-boost matrix converter," *IEEE Trans. Power Electron.*, vol. 25, no. 2, pp. 453– 462, Feb. 2010.

[31] M.-K. Nguyen, Y.-G. Jung, and Y.-C. Lim, "Single-phase AC/AC buck-boost converter with single phase matrix converter topology," in *Proc. Eur. Conf. Power Electron. Appl.*, 2009, pp. 1–7.

[32] Y.-D. Yoon and S.-K. Sul, "Carrier-based modulation technique for matrix converter," *IEEE Trans. Power Electron.*, vol. 21, no. 6, pp. 1691–1703, Nov. 2006.

[33] B. Chen, B. Gu, L. Zhang, Z. U. Zahid, J.-S. Lai, Z. Liao, and R. Ho, "A high-efficiency MOSFET transformer less inverter for nonisolated microinverter applications," *IEEE Trans. Power Electron.*, vol. 30, no. 7, pp. 3610–3622, Jul. 2015.

[34] H. F. Ahmed, H. Cha, Z. Aleem, A. A. Khan, and H.-G. Kim, "A novel buck-boost ac-ac converter with inverting and non-inverting operation and no commutation problem" in *Proc. IEEE Int. Conf. Power Electron. ECCE Asia*, 2015, pp. 920–926.

[35] H. F. Ahmed, H. Cha, A. A. Khan, and H.-G. Kim, "A novel buck-boost ac-ac converter with both inverting and non-inverting operations and without commutation problem," *IEEE Trans. Power Electron.*, vol. 31, no. 6, pp. 4241–4251, Jun. 2016.

Hafiz Furqan Ahmed received the B.S. degree in electronics engineering from the National University of Sciences and Technology, Islambad, Pakistan, in 2012. He is currently working toward the M.S. degree leading to the Ph.D. degree at the School of Energy Engineering, Kyungpook National University, Daegu, South Korea.

His current research interests include high-efficiency bidirectional dc–dc converters, ZS inverters, and high-reliable ac–ac converters without commutation problem.

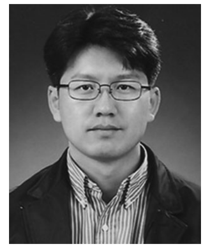

Honnyong Cha (S'08–M'10) received the B.S. and M.S. degrees in electronics engineering from Kyungpook National University, Daegu, South Korea, in 1999 and 2001, respectively, and the Ph.D. degree in electrical engineering from Michigan State University, East Lansing, MI, USA, in 2009.

From 2001 to 2003, he was a Research Engineer with the Power System Technology Company, An-san, South Korea. From 2010 to 2011, he was a Senior Researcher with the Korea Electrotechnology Research Institute, Changwon, South Korea. In 2011, he joined the School of Energy Engineering, Kyungpook National University, as an Assistant Professor. His current research interests include high-power dc–dc converters, dc–ac inverters, ZS inverters, and power conversion for electric vehicles and wind power generation.

Ashraf Ali Khan received the B.E. degree in electronics engineering from the National University of Sciences and Technology, Islambad, Pakistan, in 2012. He is currently working toward the M.S. degree leading to the Ph.D. degree at the School of Energy Engineering, Kyungpook National University, Daegu, South Korea.

His current research interests include magnetics, buck–boost inverters, solid-state transformer, and ac–ac converters.

Juyong Kim received the M.S. and Ph.D. degrees from Kyungpook National University, Daegu, South Korea, in 1994 and in 2007, respectively.

In 1994, he joined the Korea Electric Power Corporation Research Institute, Daejon, South Korea, as a Researcher, where he is currently a Principal Researcher at the Smart Power Distribution Laboratory. His main research interests include dc distribution system and dc microgrid.

Jintae Cho received the B.S. and M.S. degrees in electrical engineering from Korea University, Seoul, South Korea, in 2006 and 2008, respectively, where he is currently working toward the Ph.D. degree in dc distribution.

He is currently a Senior Researcher at the Smart Power Distribution Laboratory, Korea Electric Power Corporation Research Institute, Daejeon, South Korea. His research interests include protection, monitoring, and control of LVdc distribution system.